21st Australasian Fluid Mechanics Conference
Adelaide, Australia
10-13 December 2018

Morphology Induced Variation on Nanoparticle Transport in Human Upper Tracheobronchial Airways

JW Ma[1], YD Shang[1], L Tian[1] and JY Tu [1]

[1]School of Engineering – Mechanical and Automotive
RMIT University, Victoria 3083, Australia

Abstract

Nanoparticle transport and deposition in human lung has attracted considerable attention in past few decades, as it has significant value to the understanding of inhalation toxicity consequence as well as therapeutic potential in occupational health and medical applications. First task of such study is to rebuild the respiratory system, most closely resemble the physical and physiological features. In reproducing human tracheobronchial airways, two approaches were frequently employed, that are: 1) anatomical realistic reconstruction through image scans (e.g. CT and MRI) or via cadaver casts; 2) mathematical description using simplified models. Strengths and limitations are primarily on accuracy, resolution, repeatability, and computational expenses. While studies using both approaches have been reported in the literature, detailed comparison of nanoparticle transport and deposition in the two representations were scarcely performed, largely due to the challenge to acquire comprehensive data from the irregular structured airway replicas (approach 1), and the computational expenses. To fill the gap, current study performed a numerical comparison of nanoparticle transport and deposition in human upper tracheobronchial airways by using an anatomical realistic reconstruction (through CT scans) and a mathematical simplified airway model. As the first step, current study was focused on the variation in breathing airflow pattern, and the effect towards fate of the inhaled nanoparticles in human upper tracheobronchial airways (trachea and the first bifurcation). The study provided important information to understand the geometry induced sensitivity of nanoparticle modelling in human tracheobronchial airway, and is of significant value to predict whole lung uptake of inhaled nanoparticles in human respiratory systems.

Introduction

The study of aerosol transport and deposition in human respiratory system involves airway model rebuild, air conditioning performance analysis, and particle deposition evaluations. Human respiratory system consists of the extrathoracic airways (nasal cavity, pharynx and larynx), lung and respiratory alveolar ducts, responsible for air exchange and particle removal along with many other functions. Due to significant irregularity, extrathoracic airways are frequently reconstructed via image scans or cadaver casts[1, 11], whereas for tracheobronchial and alveolar airway branches, mathematical description is favoured as it offers greater assembling flexibility and computing efficiency[3, 10]. With human tracheobronchial tree containing millions of branches tailored to its physiological function, whole lung modelling can only be accomplished through stochastic protocols guided by main branching features obtained from airway samples [7]. With this approach, Weibel [12] prescribed a symmetric planar human lung morphometry covering all 23 generations with branching details quantified by mathematical equations. Further improvements were made by subsequent researchers accounting for asymmetry and the out-of-plane morphologies [7]. It should be noted that, while whole lung modelling unanimously took the mathematical route, anatomical realistic reconstruction from CT/MRI scans or cadaver casts were also used in the study of transport phenomenon in regional tracheobronchial trees [13].

By adopting both anatomical reconstructed and mathematical generated models to investigate transport phenomenon in human tracheobronchial airways, a systematic comparison of the transport outcome were scarcely performed. Morphology induced variation is anticipated, however, to what extent and on what ground have not been fully studied. On the other hand, correlations of the two representations in determining flow and particle dynamics could provide critical information to understand the transport process and provide solid ground to assess whole lung modelling efficacy.

Apart from direct comparison to seek morphology induced variation in transport processes, some of the inhalation simulation study in human tracheobronchial airways focused on flow and particle dynamics most accurately replicate the resistance, energy consumption, and particle fate of various practical applications. By viewing human tracheobronchial tree as sequence of connected bifurcating passages, Tian and Ahmadi [10] reconstructed the first four generation by fusing a sequence of base bifurcating elements on prescribed physiological realistic mathematical description [3]. Micro- and Nano- particle transport and deposition were investigated, and the simulated deposition efficiency in trachea and the first three bifurcations were comparable to the experimental measurement [13]. Although their study provided valuable insight towards the regional flow and particle dynamics in human tracheobronchial airways, a comprehensive morphology effect on nanoparticle transport cannot be inferred. With the advancement of nanotechnology and an increased interest on nanoparticle transport in human respiratory system, such information is of significant importance.

With an anatomically reconstructed model via CT scans and a mathematically generated airway model, this study performs a detailed numerical comparison of nanoparticle transport and deposition in human upper tracheobronchial airways. At this stage, the research focused on the variation in breathing airflow pattern induced by anatomical morphology features such as surface roughness, airway morphology, cross-sectional profiles and branching angles. The effect towards inhaled nanoparticles was also investigated. This research provides an in-depth understanding of toxicity consequence of inhaled small particles, as well as valuable information towards therapeutic design in terms of targeted drug delivery systems.

Method

Human upper tracheobronchial airway geometric models

The anatomical realistic human respiratory system with major tracheobronchial tree was reconstructed via segmentation technique using CT scans of a 43 year old healthy male (Hubei Cancer Hospital, Wuhan, China). Further details on model reconstruction and verification can be found in the work of Inthavong et al. [6].

Current study focused on trachea, and the main bronchus leading to the left and right lung. The truncated airway shown in Figure 1 initiated from trachea entrance and existed at

openings of the secondary bronchi, including the three right and two left lobes respectively. Short artificial extension toward the head airway was joined to the trachea to form a contiguous pathway for future integrated study. Key geometric features of the truncated airway were given in Figure 1, which defined the main branching outline such as airway cross sectional diameters, airway lengths, and the branching angles. It should be noted that, rather than being circular and smooth, cross sections of the trachea were wavy and predominantly crescent-shaped with cartilaginous rings uniformly spaced to support the airway. As the anatomical cross section is non-circular, diameter in Figure 1 was defined as the average of the maximum and minimum span of the cross sectional area in the tracheobronchial airways [4].

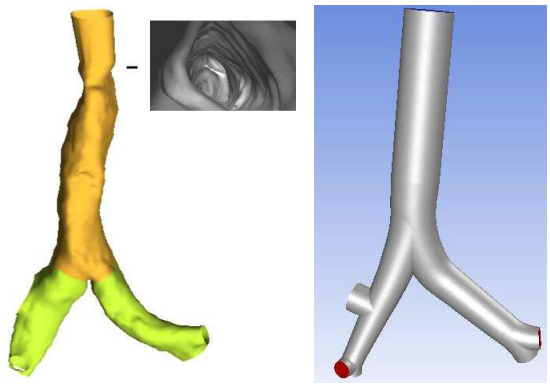

Figure 1. Schematic of the human airway geometric model: (Left) anatomical realistic human tracheobronchial airway reconstruction (CT scans); (Right) reconstructed mathematical simplified airway model.

Mathematical simplified airway model was constructed based on the anatomical outline, where airway branches were modelled as idealized circular tubes with fine features such as surface roughness, cartilaginous rings, and oblate distortion neglected. The simplified model ensured smooth transition between airway generations. It is shown from Figure 1 that, the idealized airway conformed to the main features of the anatomical replica; however, airway curvature and deviation of airway morphology to that of straight tubes were not considered.

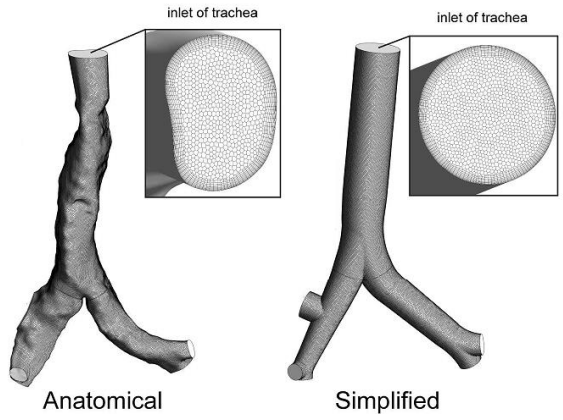

Figure 1. Computational mesh with polyhedral meshing schemes

Fluent Meshing (ANSYS 18.0) was used to generate the computational mesh (Figure 2). The resulting mesh consisted of 789,310 elements and 3,364,729 faces for the anatomical model, 692,446 elements and 3,111,176 faces for the mathematical simplified representation. Mesh independency was conducted and achieved at the specified size.

Boundary condition

Current study employed a steady inhalation model with the assumption that particle deposition mainly occurs during the inhalation phase [5]. Therefore, a steady inhalation case with 30 L/min average volume flow rate was adopted in this research. According to Tian and Ahmadi [10], laryngeal induced turbulence propagates in trachea and the first two bifurcations before fully dissipated; therefore, breathing air in current study was in turbulent state. Reynolds stress transport model (RSTM) together with the "two-layer zonal" boundary condition was shown to bring the most accurate particle deposition prediction [9, 10], and therefore was used in the current study.

Airflow was simulated using Fluent (ANSYS 18.0). The flow was driven by pressure gradient between entrance of the trachea and bronchi exists. A steady breathing was imposed with assumption of equal pressure drop at the five lobar bronchi exits. Further details of fluid flow modelling can be found in the work of Tian and Ahmadi [10].

Particle transport simulation

In this study, particles were uniformly released from the entrance of trachea. Statistically independent 100,000 uniform concentrated mono-dispersed ultrafine particles of 1, 1.1, 1.2, 1.3, 1.4, 1.5, 1.7, 2, 3, 5, 10, 15, 20, 30, 40, 50, 70 and 100 nm, were released. Deposition onto the respiratory walls occurred when the particle was within radius distance away from the airway surface.

During the numerical simulation, Lagrangian particle tracking method was used where individual particle trajectory was computed.

The particle equation is:

$$\frac{du_p}{dt} = \frac{1}{C_c}F_D + \frac{g(\rho_p - \rho)}{\rho_p} + F_L + F_B \qquad (1)$$

Where u_p stands for particle velocity, t is time, g is gravitational constant, ρ_p is the density of particle, C_c is the Cunningham correction. In this study, both gravitational and buoyancy forces can be neglected. F_D is the drag force given by $18\mu(u_p - u)/(d^2\rho_p)$, d is the particle diameter.

Particle deposition efficiency (*DE*) is defined as the ratio of the deposited particles in a region to the total number entering nasal cavity.

$$DE = \frac{\#deposited\ particles}{\#particles\ entered\ in\ the\ nasal\ cavity}$$

It is an important parameter characterizing the regional filtering capacity and particle penetration rate. Deposition efficiency (*DE*) is closely related to the transport mechanisms and for nanoparticles, size, diffusivity and airflow rate are the governing parameters. Due to the geometric complexity of human airways, no analytical expression is available for deposition efficiency (*DE*). Frequently, empirical fitted equations are used to relate measured data (*DE*) to the governing parameters.

Results and Discussion

Breathing airflow pattern

Figure 3 displayed the stream-wise airflow pattern at 30 L/min breathing rate in central plane of the tracheobronchial airways. Simulation results from anatomical and idealized geometries were plotted side by side for comparison. As shown in the graph, flow development in trachea of the idealized model was smooth, with parabolic profiles gradually formed due to

boundary no slip condition. The flow partitioned at the carina ridge with distortions to enter subsequent branches asymmetrically.

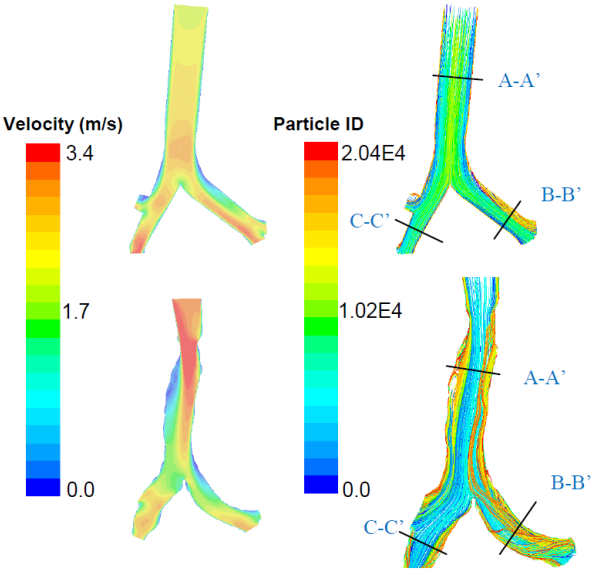

Figure 3. stream-wise airflow pattern at moderate breathing in central plane of the tracheobronchial airways: (Left) velocity magnitude; (Right) flow pathlines.

The data showed strong mixing in the anatomical model corresponding to the observation in Figure 3. While the secondary flow in the idealized model was mainly induced by formation of the boundary and flow partition at the bifurcations, geometry irregularity in the anatomical model was also a major contribution.

Wall shear stress

Table 1 listed the averaged wall shear stress in trachea, left and right bronchi in the idealized and anatomical models. It was seen that, while anatomical model exhibited higher stress in the trachea (24.2%), wall shear of the left and right bronchi was higher in the idealized model (26.8% and 9.5%). Wall shear distribution could well indicate the level of secondary flow and forming of local eddies contributing to enhancement of the particle deposition.

	Wall Shear Stress (Pa)		
	Trachea	Bronchi (L)	Bronchi (R)
Idealised	0.069	0.104	0.288
Anatomical	0.091	0.082	0.277

Table 1. Wall shear stress distribution in the airway models

Particle deposition efficiency

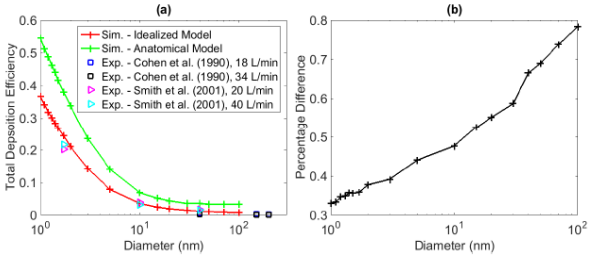

Figure 4. Total deposition efficiency in the airway models: (a) comparison with experiments; (b) percentage difference between anatomical realistic and idealized models.

Figure 4a displayed the total deposition efficiency of the released particles in truncated tracheobronchial airway models. Experimental measurement on nanoparticle deposition in human tracheobronchial airway casts by Cohen et al. [2] and Smith et al. [8] were plotted for comparison. In the respective experiments, mono dispersed particles of ferric oxide and 212Pb at breathing rates of 18, 34, 20 and 40 L/min were considered. It was shown in Figure 4 that, for the range of particles studied, deposition efficiency decreases with the increase of particle size; therefore, diffusion is the dominant transport mechanism. While general trends agree, anatomical model captured considerable more particles than that of the simplified representation (33% to 78%, Figure 4b). The experimental measurement [2, 8] was in reasonable agreement with simulation, and appeared to match more of the prediction by using the mathematical simplified model. Figure 4b displayed the percentage difference of the simulated deposition efficiency between anatomical and idealized models and variation in the range of 33% to 78% was exhibited. It was interesting that while large variation in magnitude was observed with smaller sized particles, the percentage difference was monotonically increasing between the two models as the particle size grows. This implied a higher morphology dependency of larger sized nanoparticles in the transport process.

Figure 5 compared the regional deposition efficiencies in trachea, left and right bronchi in the anatomical and idealized models. Remarkable similar level of depositions were observed in the secondary branches (Figure 5b and 5c), while deposition efficiency in the trachea was considerably different. Anatomical model collected considerable more particles in the trachea than that in the idealized model. In connection with Figure 4, it was clear that variation in the total deposition efficiency between the two geometric models was mainly contributed by trachea deposition.

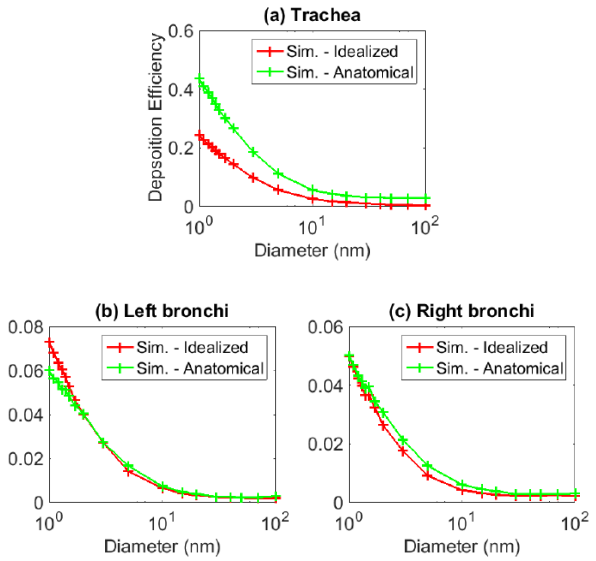

Figure 5. Regional deposition efficiency in the airway models: (a) trachea; (b) left bronchi; (c) right bronchi.

Figure 6 displayed the partition (percentage) of the particles that succeeded to enter the next level airway branch through the left and right bronchi. It was seen from the figure that partition of the particles penetrated to the next level was about 45% to 55% between the left and right bronchi for both the anatomical and idealized models. However, consistently more percentage of the

penetrated particles went through the left bronchi in idealized geometry than that in the anatomical one.

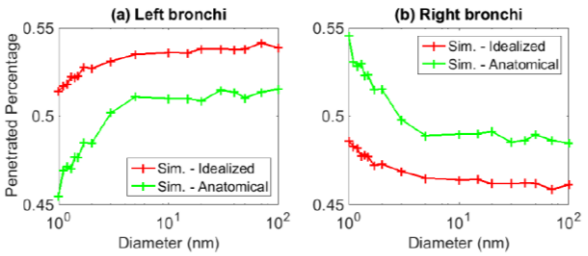

Figure 6. Percentage of the particles penetrated to the next level tracheobronchial tree through: (a) left bronchi; (b) right bronchi.

A remarkable correlation between the flow and particle partitions (Table 2, Figure 6) was identified for the 1nm particles where about 51% went through the left bronchi and 49% to the right in the idealized model. For the anatomical model, about 42% went through the left bronchi and 58% to the right. As the particle size increased, correlation became weakened and the left and right proportion approached to each other for the anatomical model, while they departed further away in the idealized model. One explanation would be higher sensitivity to the airway morphology for larger sized nanoparticles, where the shear and secondary flow enhanced the mixing as particles travelled downstream.

	Volume Flow Rate (L/min)					
	Trachea		Bronchi (L)		Bronchi (R)	
Idealised	30	100%	15.32	51%	14.68	49%
Anatomical	36	100%	12.56	42%	17.44	58%

Table 2. Flow partition in the airway models

Conclusions

In this study, a numerical comparison was conducted between an anatomical realistic reconstructed and a mathematical simplified human upper tracheobronchial airway models in terms of inhaled nanoparticle transport and deposition. By applying different fates of inhaled nanoparticles, the variation in breathing airflow pattern and the effect towards fate of the inhaled nanoparticles in human upper tracheobronchial airways were investigated. Based on the simulation results, following conclusions were drawn:

- Major irregularity at trachea and head airway connection induced significant disturbances to the airflow, turbulence, wall shear and secondary flow distributions;
- Particle transport in secondary bronchi performed less sensitivity towards morphology induced disturbance; To some degree, deposition was more related to wall shear stress while penetration was more affected by turbulence and secondary flow mixing;
- Nanoparticle deposition in the anatomical model was considerably higher than that in the simplified model mainly due to enhanced deposition in the trachea; nanoparticle deposition in bronchi of the anatomical and idealized models were comparable;
- Effect of morphology on nanoparticle transport and deposition in human tracheobronchial airways is stronger for larger sizes than the smaller ones;
- Further investigation is required in regards to morphology sensitivity in human airway particle transport modelling.

Acknowledgements

The financial supports provided by the National Natural Science Foundation of China (Grant no.91643102) and the Australian Research Council (Project ID: DP160101953 and DE180101138) are gratefully acknowledged.

References

1. Cheng, Y.-S., Y. Zhou, and B.T. Chen, *Particle deposition in a cast of human oral airways.* Aerosol Science & Technology, 1999. **31**(4): p. 286-300.
2. Cohen, B.S., R.G. Sussman, and M. Lippmann, *Ultrafine particle deposition in a human tracheobronchial cast.* Aerosol Science and Technology, 1990. **12**(4): p. 1082-1091.
3. Heistracher, T. and W. Hofmann, *Physiologically realistic models of bronchial airway bifurcations.* Journal of Aerosol Science, 1995. **26**(3): p. 497-509.
4. Horsfield, K. and G. Cumming, *Morphology of the bronchial tree in man.* Journal of applied physiology, 1968. **24**(3): p. 373-383.
5. Inthavong, K., et al., *Micron particle deposition in a tracheobronchial airway model under different breathing conditions.* Medical engineering & physics, 2010. **32**(10): p. 1198-1212.
6. Inthavong, K., et al., *From CT scans to CFD modelling–fluid and heat transfer in a realistic human nasal cavity.* Engineering Applications of Computational Fluid Mechanics, 2009. **3**(3): p. 321-335.
7. Ramprasad, V.H. and D.O. Frank-Ito, *A computational analysis of nasal vestibule morphologic variabilities on nasal function.* J Biomech, 2016. **49**(3): p. 450-7.
8. Smith, S., Y.-S. Cheng, and H.C. Yeh, *Deposition of ultrafine particles in human tracheobronchial airways of adults and children.* Aerosol Science & Technology, 2001. **35**(3): p. 697-709.
9. Tian, L. and G. Ahmadi, *Particle deposition in turbulent duct flows—comparisons of different model predictions.* Journal of Aerosol Science, 2007. **38**(4): p. 377-397.
10. Tian, L. and G. Ahmadi, *Transport and deposition of micro-and nano-particles in human tracheobronchial tree by an asymmetric multi-level bifurcation model.* The Journal of Computational Multiphase Flows, 2012. **4**(2): p. 159-182.
11. Tu, J., K. Inthavong, and G. Ahmadi, *Computational fluid and particle dynamics in the human respiratory system*. 2012: Springer Science & Business Media.
12. Weibel, E.R., A.F. Cournand, and D.W. Richards, *Morphometry of the human lung*. Vol. 1. 1963: Springer.
13. Zhou, Y. and Y.-S. Cheng, *Particle deposition in a cast of human tracheobronchial airways.* Aerosol Science and Technology, 2005. **39**(6): p. 492-500.